




# Design of an Air-Fed PTC Solar Field Integrated With a Rock Bed-Based Thermal Energy Storage System

Antonio Cristaudo<sup>1,\*</sup> , Francesco Nicoletti<sup>1</sup> , Francesco Rovense<sup>2</sup> , Walter Gaggioli<sup>2</sup>,  
Vittorio Ferraro<sup>3</sup>, and Natale Arcuri<sup>1</sup>

<sup>1</sup>Department of Mechanical, Energy and Management Engineering - University of Calabria, Italy

<sup>2</sup>ENEA Casaccia Research Centre, Italy

<sup>3</sup>Department of Computer, Modelling, Electronics and System Engineering - University of Calabria, Italy

\*Correspondence: Antonio Cristaudo, [antonio.cristaudo@unical.it](mailto:antonio.cristaudo@unical.it)

**Abstract.** Integrating solar energy to provide heat for industrial processes represents a viable solution aligned with the ongoing energy transition. Parabolic trough collectors (PTCs) are a reliable and mature technology within this context. This study addresses the performance of an industrial air-drying plant integrated with a PTC solar field and a thermal energy storage (TES) system comprising two rock beds operating in parallel. To improve the exploitation of solar radiation, pressurized air was used as the heat transfer fluid for the PTC due to its high temperature limits. A parametric analysis was conducted to evaluate the impact of solar field size on performance, varying both the number of modules in series per string and the number of parallel strings. Results show that the solar fraction (SF) increases with the number of parallel strings, while increasing the number of series modules initially raises the SF to a peak before slightly decreasing. The maximum SF achieved was 85% with a TES volume of 96.24 m<sup>3</sup> and a solar field comprising 12 modules in series and 4 parallel strings, resulting in a total collection area of 3450 m<sup>2</sup>.

**Keywords:** Solar Energy, Parabolic Trough Collector, Industrial Process Heat, Drying, Rock Bed.

## 1. Introduction

The goal of achieving fossil fuel independence has long been shared among major industrial nations [1]. The energy crisis and the urgent need to mitigate climate change have intensified interest in sustainable solutions [2]. According to the IEA, the industrial sector consumes about 30% of global energy, with medium to high-temperature applications (200–600°C) accounting for roughly 70% of industrial thermal energy use. This significant market share underscores the relevance of parabolic trough collectors (PTCs), the most advanced and cost-effective technology for large-scale solar energy applications [3]. PTCs also feature single-axis sun tracking, enhancing solar radiation capture by 30% compared to fixed devices [4]. Common heat transfer fluids (HTFs) include thermal oils and molten salts; however, thermal oils do not allow for high temperatures and raise safety and toxicity concerns, while molten salts, stable up to 600°C, require careful management to remain liquid and avoid freezing [5]. Air offers a high-temperature, high-pressure alternative [6]. Indeed, by using air, which is a non-toxic and cost-free HTF, allows for temperatures up to 1300 K at the solar field's outlet [7]. This feature minimizes disruptions during high solar radiation periods, thereby increasing the solar fraction [8]. Additionally, a higher maximum temperature shortens the charging time for a given storage

volume. Indeed, to address the intermittency of solar sources, solar-powered systems often integrate a TES [9]. While most commercial Concentrating Solar Thermal (CST) plants with TES use thermal oils or molten salts in a two-tank configuration, rock beds (RBs) present advantages like material abundance, cost-effectiveness, and wide temperature range applicability, allowing direct heat transfer between the working fluid and storage media. Literature includes various studies on integrating PTC systems with TES for Industrial Process Heat (IPH) applications. Akba *et al.* [10] dynamically simulated a PTC solar field with two molten salt storage tanks for process heat, providing a sizing methodology based on the solar fraction. Kalogirou [11] assessed the performance of a water-based PTC feeding a storage tank for industrial heat supply. Silva *et al.* [12] analysed the techno-economic performance of a PTC system integrated into an industrial process, optimizing the solar field and storage tank dimensions. Othman *et al.* [13] modeled and experimentally validated a system where an oil-based PTC heats a storage tank, with an oil-to-air heat exchanger used to dry sludge from olive mills. Silva *et al.* [8] studied PTC integration for steam generation in a food industry requiring saturated steam at 7 bar, with an annual consumption of 148 MWh. The system included a solar field with Therminol 55 as the HTF, a storage tank, and a steam generator. To the best of the authors' knowledge, no studies have explored a system that combines a pressurized air PTC solar field with a TES featuring two rock beds. This system is designed to heat ambient air for pasta drying in an open loop configuration within the food industry. The presence of two parallel storage volumes enables the simultaneous supply of thermal load from one rock bed and energy storage from the solar field in the other. The objective of this study is to assess the use of a dual rock bed heat storage system powered by air-fed PTC solar field. Its advantages include the ability to achieve very high temperatures. Although this solution may be less efficient in terms of collector thermal performance, this plant allows storing, for a given volume, a great amount of sensible energy within the rock beds. Furthermore, direct heat exchange within the rock bed allows for the discharge of the tank down to the temperature required by the thermal process. The air thus enables flexible operation over a wide temperature range. This study evaluated the system's performance by analyzing different configurations of the PTC modules in series and parallel. The system modeling was conducted using TRNSYS software integrated with Matlab® for thermodynamic modeling of the dryer and the control strategy implementation. The article is structured as follows: Section two describes the plant layout and its main components, the numerical model, and the control strategy. Section three presents the results of the annual SF analysis. Finally, section four outlines the conclusions and future developments.

## 2. Materials and Methods

### 2.1 System and Component Description

The entire system comprises a heat generation section and a utilization section, with a nominal load of 120 kW, both managed through a control logic. The interface component between the two sections is the TES system, represented by two rock beds of the same size, operating in parallel during both charging and discharging phases. Figure 1 depicts the proposed plant in one of its operational configurations and its main components.

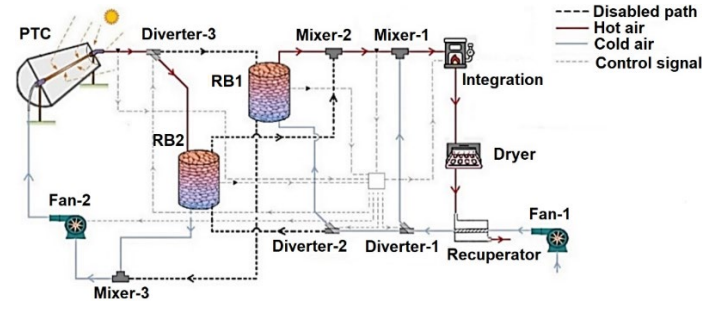


**Figure 1.** Power plant layout and main components.

The generation section features a closed loop where air at 10 bar pressure circulates through the solar field [14],[15]. As the air passes through the PTC, it heats up, and diverter-3 directs it to the rock bed in the charging phase. In the utilization section, diverter-2 directs ambient air to the rock bed in the discharging phase. The hot air flows through the dryer, transfers part of its sensible heat to incoming air, and is then expelled, as is typical in food industry applications [11]. This study assumes that the dryer operates continuously, as is typically the case in large-scale industrial applications [12]. If the storage system does not have sufficient energy to meet the dryer's temperature requirements, diverter-1 directs the incoming air to the auxiliary heater. Conversely, if the air temperature exiting the RB in the discharging phase exceeds the temperature required for the dryer, diverter-1 bypasses part of the total mass flow exiting the recuperator to mix with the remaining air flow rate from the RB in mixer-1 to achieve the desired temperature for the dryer.

## 2.2 Numerical Model

To assess the energy performance of the proposed system with various solar field sizes, annual dynamic simulations were conducted using TRNSYS18 on a 15-minute time step [16]. The system components were modeled using Types 15 and 16 for climatic data, Type 74 for the solar field, Type 10 for the rock bed, Type 5 for the recuperator, Type 6 for the auxiliary heater, and Type 148 for the diverters. In the analysed case study, the climate data was based on Crotona, Italy, with the solar field set to an East-West tracking axis to achieve the best performance throughout the year [17], [18]. The dryer was modeled in Matlab® as an adiabatic environment maintained at 90°C by using the energy and mass balance equations [19]:

$$\dot{m}_{dryer} \cdot h_{air,I} + \dot{m}_p \cdot h_{p,I} + \dot{m}_w \cdot h_{wp,I} = \dot{m}_{dryer} \cdot h_{air,O} + \dot{m}_p \cdot h_{p,O} + \dot{m}_w \cdot h_{wp,O} \quad (1)$$

$$\dot{m}_{w,I} - \dot{m}_{w,O} = \dot{m}_p \cdot (\phi_{p,I} - \phi_{p,O}) = \dot{m}_{dryer} \cdot (X_{air,O} - X_{air,I}) \quad (2)$$

where  $X_{air}$  is the absolute humidity of the air, with  $h_{air}$ ,  $h_p$ , and  $h_{wp}$  representing the enthalpies of drying air, pasta, and water in the pasta, respectively. The model's unknowns are the processed mass flow rate and the exiting air's absolute humidity. The pasta's specific heat was set at 2.485 kJ/kg K, with inlet and outlet temperatures of 52°C and 44°C, indicating thermal equilibrium between the pasta and its water content [19], [20]. It was assumed that an air flow rate of 5 kg/s passes through the dryer, transferring sensible heat and absorbing moisture due to the evaporation of the water content ( $\phi_p$ ) from the processed pasta flow rate. The water content in the pasta must be reduced from 30% to 11% by weight, in accordance with national regulations [19]. The air enters the dryer at an inlet temperature of 110 °C, as required by the user. This temperature is chosen to efficiently transfer heat to the water in the pasta and to lower the relative humidity compared to ambient conditions, thereby enhancing the mass transfer process. The TES system consists of two RB filled with quartz, as this material provides thermal stability up to temperatures of 1000 °C and is suitable for storage in CSP applications [21]. To minimize thermal losses to the environment, it was assumed that each RB is insulated and has a global heat loss coefficient of 0.28 W/m<sup>2</sup>·K [13]. The TES volume was sized by

considering that the stored energy must cover the daily energy requirement of the dryer over 24 hours. The minimum temperature achievable during the discharge phase was set to the inlet temperature required by the dryer, while the maximum temperature to which the RB can be charged was set at 400 °C. This value strikes a balance between minimizing storage volume and limiting thermal losses to the external environment. The assumed void fraction is 0.3, while the density, specific heat, and thermal conductivity are 2500 kg/m<sup>3</sup>, 0.8 kJ/kg·K, and 3.0 W/m·K, respectively [22]. This study assumes that the maximum temperature achievable by the air exiting each collector series is limited by the absorber tube material's maximum allowable temperature [23]. To identify the highest air temperature before the control system interrupts the solar field feed, the Gnielinski correlation for gaseous fluids was iteratively applied at the tube's outlet to calculate the convective heat transfer coefficient [14], [24].

$$h = \left\{ \frac{(\xi/8) \cdot (Re - 1000)}{1 + 12.7 \cdot \sqrt{(\xi/8) \cdot (Pr^{2/3} - 1)}} \cdot \left[ 1 + \left( \frac{D_{in}}{L} \right)^{2/3} \right] \cdot \left( \frac{T_w}{T_{air}} \right)^n \right\} \cdot \frac{k_{air}}{D_{in}} \quad (3)$$

where  $D_{in}$ ,  $L$ ,  $Re$ ,  $Pr$ ,  $k_{air}$  and  $\xi$  represent the inner diameter of the tube, tube length, Reynolds number, Prandtl number, thermal conductivity of air and friction factor, respectively. For further clarification, see Ref. [14].  $T_w$  and  $T_{air}$  are the temperature of the inner surface of the absorber and the temperature of the air in the considered section, respectively. Adopting a conservative approach, the maximum thermal flux incident on the absorber tube ( $\Phi_{max}$ ) was calculated by considering the maximum Direct Normal Irradiance ( $DNI_{max}$ ) of 990 W/m<sup>2</sup> incident on the parabolic PTC mirrors at the specified location, while convective and radiative losses from the absorber were neglected.

$$\phi_{max} = DNI_{max} \cdot \cos(i) \cdot \rho_{mirr} \cdot \tau_{env} \cdot \alpha_{abs} \cdot \gamma \cdot \frac{A_{par}}{A_{abs}} \quad (4)$$

Each assembly's module has an aperture width of 5.75 m, a length of 12.5 m, and a  $D_{in}$  of 0.076 m. The mirror reflectivity ( $\rho_{mirr}$ ), glass envelope transmissivity ( $\tau_{env}$ ), receiver absorptance ( $\alpha_{abs}$ ), and tracking error factor ( $\gamma$ ) are 0.94, 0.96, 0.95, and 0.92, respectively [25], [26]. Finally,  $A_{par}$  represents the gross area of the parabolic mirrors, while  $A_{abs}$  is the area of the absorber tube. At this stage, the expression for  $T_w$  is derived as a function of the convective heat transfer coefficient by equating the maximum thermal flux to the convective thermal flux exchanged between the absorber tube and the heat transfer fluid [27].

$$T_w = \frac{\phi_{max}}{h} + T_{air} \quad (5)$$

By substituting Eq. (5) into Eq. (3), the value of  $T_{air}$  was varied iteratively until the corresponding value of the convective heat transfer coefficient  $h$  provided a  $T_w$  value within the material's limits. AISI 316L stainless steel, commonly used in PTC absorber tubes, was selected for its high melting point of 1400°C and maximum operating temperature of 1100°C [28]. The absorbers were coated with Pyromark 2500, which can withstand up to 1000°C [25]. Through iterative testing, the outlet air temperature ( $T_{air,out,max}$ ) was found to reach 867°C, with a wall temperature of 986°C. Using the ideal gas law, the air density at these temperatures and operating pressures was calculated, allowing for the determination of the air mass flow rate for each collector string as per Eq. (6):

$$\dot{m}_{air} = \rho_{air,out} \cdot \left( \frac{D_{in}^2}{4} \right) \cdot v_{max} \quad (6)$$

For air temperatures up to 867 °C at the PTC outlet, this mass flow rate is the maximum that ensures the fluid velocity exiting each string—and therefore throughout all other sections of the tube—stays below the 20 m/s velocity limit [16]. This results in a maximum air mass flow rate per string of 0.28 kg/s. The parametric analysis considered solar field configurations with 1, 2, and 4 collector strings in parallel. For each configuration, the number of modules in series per string varied from 4 to 20, increasing in increments of 4. To evaluate the system's performance as a function of solar field size, the SF was defined as the ratio of the annual energy

saved from conventional sources through the proposed system to the annual energy that would have been required to supply the same thermal load using a conventional drying system ( $E_{load}$ ).

$$SF = \frac{E_{load} - E_{aux}}{E_{load}} \quad (7)$$

## 2.3 Control Strategy

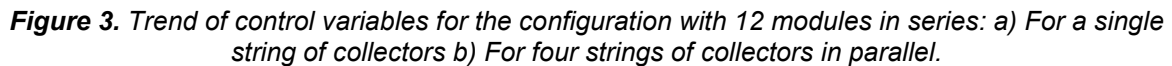
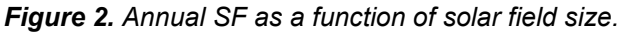
The TES system facilitates operational continuity by allowing one RB to be charged with hot air from the PTC while the other RB simultaneously discharges to supply the dryer. The controlled components within this system perform key functions to maintain this balance. Diverter-1 diverts part of the air mass flow rate from the recuperator to Mixer-1 if the temperature from the discharging RB exceeds the set-point temperature for the dryer; if neither RB can discharge, Diverter-1 redirects all airflow to the auxiliary burner. Diverter-2 and Diverter-3 manage the airflow to support the discharging and charging phases of the two rock beds, respectively. Meanwhile, Fan-2 either enables or disables the solar field supply based on the control signals. The control system defines the states of the valves, and the fan based on the state of charge (SOC) of the RB and the outlet temperature of the heat transfer fluid from the solar field ( $T_{OUT\_PTC}$ ). In particular, to evaluate the charge level of the rock bed, the state of charge (SOC), assessed based on the average temperature  $T_{RB}$  evaluated at various points along the height of the rock bed, was defined as:

$$SOC = \frac{T_{RB} - T_{RBmin}}{T_{RBmax} - T_{RBmin}} \quad (8)$$

where  $T_{RBmin}$  and  $T_{RBmax}$  represent the minimum allowable temperature of the rock bed during discharge, and the maximum temperature at which the rock bed can be charged, respectively. To effectively charge the designated rock bed, the  $T_{OUT\_PTC}$  must fall between the RB's temperature and the maximum allowable air temperature. To minimize frequent switching between operational phases, lower and upper deadbands are set at 5% and 95% of the SOC, respectively. If both rock beds have a SOC within the 0-100% range, no switching occurs, and each continues in its current phase, either charging or discharging. However, if the RB in the charging phase reaches a 100% SOC, it only switches to discharging when the other rock bed's SOC falls below 95%, during which the PTC is shut down. Conversely, if the discharging RB reaches a 0% SOC, it is enabled for charging once the other's SOC reaches at least 5%, with the dryer being powered by the auxiliary heater up to that point.

## 3. Results and Discussion

Figure 2 presents the annual solar fraction results, analyzed by the number of modules connected in series per string and varying the number of strings in parallel, representing the total air flow rate in the closed loop. Each collector string handles an air flow rate of 0.28 kg/s, and each rock bed has a storage volume of about 48 m<sup>3</sup>.



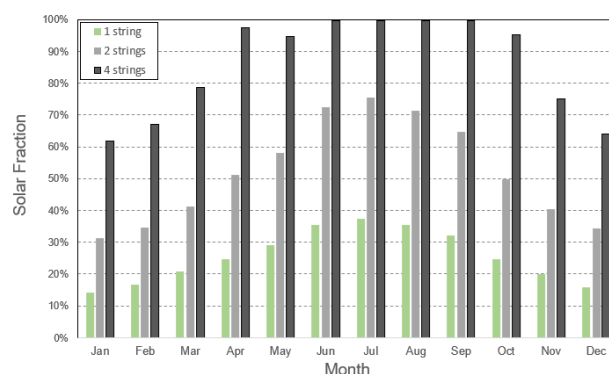


Figure 4. Monthly SF for 12-module series strings

## 4. Conclusions

This study explored a novel PTC solar system integrated with a TES consisting of two rock beds for an industrial pasta drying process that requires a constant thermal power of 120 kW. The system utilized pressurized air as HTF, achieving temperatures up to 867°C without disrupting the solar field's operation. The dual rock bed TES facilitated both the simultaneous supply and storage of thermal energy from the solar field. Moreover, the added value of using the dual rock bed storage system, and thus the direct use of air for both the charging and discharging phases, lies in the ability to exploit a wide temperature difference within the storage tank. Indeed, if molten salts were used as the HTF, it would not be feasible to cool the storage tank during the discharge phase to temperatures close to those required by the user, due to the limitations imposed by the high melting point. Even when using thermal oil, however, the system would still require a secondary circuit with additional heat exchange systems to transfer the thermal power to the dryer, adding complexity to the plant. To assess the system's efficacy, fifteen dynamic simulations were conducted using the solar fraction as the primary performance metric. The findings indicated that the SF improved with an increase in both the number of modules per string and the number of parallel strings. The optimal system configuration—comprising 12 modules in series and four parallel strings—achieved an 85% solar fraction, with a total airflow rate of 1.12 kg/s and a collector area of 3450 m<sup>2</sup>. Notably, during the summer months, this configuration successfully satisfied the thermal demand of the dryer. Further works will include a techno-economic analysis to calculate the Levelized Cost of Heating (LCOH) as a function of the storage and solar field sizes, aiming to determine the most cost-effective configuration.

## Data availability statement

Data will be made available on request.

## Author contributions

**Antonio Cristaudo:** Methodology, Writing – original draft, Visualization, Software, Data Curation. **Francesco Nicoletti:** Methodology, Conceptualization, Writing – review & editing. **Francesco Rovense:** Methodology, Writing – review & editing. **Walter Gaggioli:** Supervision. **Vittorio Ferraro:** Resources, Supervision. **Natale Arcuri:** Supervision, Project Administration.

## Competing interests

The authors declare that they have no competing interests.

## Funding

This research was conducted as part of the NEST Project (Network 4 Energy Sustainable Transition), CUP F53C22000770007, National Recovery and Resilience Plan (NRRP), Mission 4, Component 2, Investment 1.3 and partly funded under the NRRP, Mission 4, Component 1, Investments 3.4, 4.1 - Call for tender No. 118 of 2023 of Italian Ministry of University and Research funded by the European Union – NextGenerationEU.

## References:

- [1] A. Manasrah, M. Masoud, Y. Jaradat, and P. Bevilacqua, "Investigation of a Real-Time Dynamic Model for a PV Cooling System," *Energies*, vol. 15, no. 5, p. 1836, Mar. 2022, doi: [10.3390/en15051836](https://doi.org/10.3390/en15051836).
- [2] R. Bruno, N. Arcuri, and C. Carpino, "The Passive House in Mediterranean Area: Parametric Analysis and Dynamic Simulation of the Thermal Behaviour of an Innovative Prototype," *Energy Procedia*, vol. 82, pp. 533–539, Dec. 2015, doi: [10.1016/j.egypro.2015.11.866](https://doi.org/10.1016/j.egypro.2015.11.866).
- [3] A. Ahmad, O. Prakash, R. Kaushar, G. Kumar, S. Pandey, and S. M. M. Hasnain, "Parabolic trough solar collectors: A sustainable and efficient energy source," *Materials Science for Energy Technologies*, vol. 7, pp. 99–106, 2024, doi: [10.1016/j.mset.2023.08.002](https://doi.org/10.1016/j.mset.2023.08.002).
- [4] R. Bruno, P. Bevilacqua, L. Longo, and N. Arcuri, "Small Size Single-axis PV Trackers: Control Strategies and System Layout for Energy Optimization," *Energy Procedia*, vol. 82, pp. 737–743, Dec. 2015, doi: [10.1016/j.egypro.2015.11.802](https://doi.org/10.1016/j.egypro.2015.11.802).
- [5] X. Wei, Y. Yin, B. Qin, W. Wang, J. Ding, and J. Lu, "Preparation and enhanced thermal conductivity of molten salt nanofluids with nearly unaltered viscosity," *Renewable Energy*, vol. 145, pp. 2435–2444, Jan. 2020, doi: [10.1016/j.renene.2019.04.153](https://doi.org/10.1016/j.renene.2019.04.153).
- [6] Y. Krishna, M. Faizal, R. Saidur, K. C. Ng, and N. Aslfattahi, "State-of-the-art heat transfer fluids for parabolic trough collector," *International Journal of Heat and Mass Transfer*, vol. 152, p. 119541, May 2020, doi: [10.1016/j.ijheatmasstransfer.2020.119541](https://doi.org/10.1016/j.ijheatmasstransfer.2020.119541).
- [7] E. Bellos, C. Tzivanidis, I. Daniil, and K. A. Antonopoulos, "The impact of internal longitudinal fins in parabolic trough collectors operating with gases," *Energy Conversion and Management*, vol. 135, pp. 35–54, Mar. 2017, doi: [10.1016/j.enconman.2016.12.057](https://doi.org/10.1016/j.enconman.2016.12.057).
- [8] R. Silva, F. J. Cabrera, and M. Pérez-García, "Process Heat Generation with Parabolic Trough Collectors for a Vegetables Preservation Industry in Southern Spain," *Energy Procedia*, vol. 48, pp. 1210–1216, 2014, doi: [10.1016/j.egypro.2014.02.137](https://doi.org/10.1016/j.egypro.2014.02.137).
- [9] G. Ferruzzi et al., "Concentrating Solar Power: The State of the Art, Research Gaps and Future Perspectives," *Energies*, vol. 16, no. 24, p. 8082, Dec. 2023, doi: [10.3390/en16248082](https://doi.org/10.3390/en16248082).
- [10] T. Akba, D. Baker, and A. G. Yazıcıoğlu, "Modeling, transient simulations and parametric studies of parabolic trough collectors with thermal energy storage," *Solar Energy*, vol. 199, pp. 497–509, Mar. 2020, doi: [10.1016/j.solener.2020.01.079](https://doi.org/10.1016/j.solener.2020.01.079).
- [11] S. A. Kalogirou, "Parabolic trough collectors for industrial process heat in Cyprus," 2002.
- [12] R. Silva, M. Berenguel, M. Pérez, and A. Fernández-García, "Thermo-economic design optimization of parabolic trough solar plants for industrial process heat applications with memetic algorithms," *Applied Energy*, vol. 113, pp. 603–614, Jan. 2014, doi: [10.1016/j.apenergy.2013.08.017](https://doi.org/10.1016/j.apenergy.2013.08.017).
- [13] F. Ben Othman et al., "Investigation of olive mill sludge treatment using a parabolic trough solar collector," *Solar Energy*, vol. 232, pp. 344–361, Jan. 2022, doi: [10.1016/j.solener.2022.01.008](https://doi.org/10.1016/j.solener.2022.01.008).
- [14] H. Benoit, L. Spreafico, D. Gauthier, and G. Flamant, "Review of heat transfer fluids in tube-receivers used in concentrating solar thermal systems: Properties and heat transfer coefficients," *Renewable and Sustainable Energy Reviews*, vol. 55, pp. 298–315, Mar. 2016, doi: [10.1016/j.rser.2015.10.059](https://doi.org/10.1016/j.rser.2015.10.059).
- [15] H. Agalit, N. Zari, M. Maalmi, and M. Maaroufi, "Numerical investigations of high temperature packed bed TES systems used in hybrid solar tower power plants," *Solar Energy*, vol. 122, pp. 603–616, Dec. 2015, doi: [10.1016/j.solener.2015.09.032](https://doi.org/10.1016/j.solener.2015.09.032).

- [16] Trnsys 18 Manual, Mathematical reference, Solar Energy Laboratory. University of Wisconsin, Madison.
- [17] M. Halimi, I. Outana, A. El Amrani, J. Diouri, and C. Messaoudi, "Prediction of captured solar energy for different orientations and tracking modes of a PTC system: Technical feasibility study (Case study: South eastern of MOROCCO)," *Energy Conversion and Management*, vol. 167, pp. 21–36, Jul. 2018, doi: [10.1016/j.enconman.2018.04.051](https://doi.org/10.1016/j.enconman.2018.04.051).
- [18] Y. Marif, H. Benmoussa, H. Bouguettaia, M. M. Belhadj, and M. Zerrouki, "Numerical simulation of solar parabolic trough collector performance in the Algeria Saharan region," *Energy Conversion and Management*, vol. 85, pp. 521–529, Sep. 2014, doi: [10.1016/j.enconman.2014.06.002](https://doi.org/10.1016/j.enconman.2014.06.002).
- [19] L. Brunetti et al., "Energy consumption and analysis of industrial drying plants for fresh pasta process," *Journal of Agricultural Engineering*, vol. 46, Jul. 2015, doi: [10.4081/jae.2015.478](https://doi.org/10.4081/jae.2015.478).
- [20] L. Ozgener and O. Ozgener, "Exergy analysis of industrial pasta drying process," *Int. J. Energy Res.*, vol. 30, no. 15, pp. 1323–1335, Dec. 2006, doi: [10.1002/er.1227](https://doi.org/10.1002/er.1227).
- [21] T. Baumann and S. Zunft, "Properties of granular materials as heat transfer and storage medium in CSP application," *Solar Energy Materials and Solar Cells*, vol. 143, pp. 38–47, Dec. 2015, doi: [10.1016/j.solmat.2015.06.037](https://doi.org/10.1016/j.solmat.2015.06.037).
- [22] R. Tiskatine et al., "Suitability and characteristics of rocks for sensible heat storage in CSP plants," *Solar Energy Materials and Solar Cells*, vol. 169, pp. 245–257, Sep. 2017, doi: [10.1016/j.solmat.2017.05.033](https://doi.org/10.1016/j.solmat.2017.05.033).
- [23] X. Daguene-Frick, A. Toutant, F. Bataille, and G. Olalde, "Numerical investigation of a ceramic high-temperature pressurized-air solar receiver," *Solar Energy*, vol. 90, pp. 164–178, Apr. 2013, doi: [10.1016/j.solener.2013.01.006](https://doi.org/10.1016/j.solener.2013.01.006).
- [24] V. Gnielinski, "On heat transfer in tubes," *International Journal of Heat and Mass Transfer*, vol. 63, pp. 134–140, Aug. 2013, doi: [10.1016/j.ijheatmasstransfer.2013.04.015](https://doi.org/10.1016/j.ijheatmasstransfer.2013.04.015).
- [25] A. Boubault, C. K. Ho, A. Hall, T. N. Lambert, and A. Ambrosini, "Levelized cost of energy (LCOE) metric to characterize solar absorber coatings for the CSP industry," *Renewable Energy*, vol. 85, pp. 472–483, Jan. 2016, doi: [10.1016/j.renene.2015.06.059](https://doi.org/10.1016/j.renene.2015.06.059).
- [26] System Advisor Model 2022.11.29 (SAM 2022.11.21). National Renewable Energy Laboratory, Golden, CO. Accessed: Apr. 01, 2024. [Online]. Available: <https://sam.nrel.gov>
- [27] N. Arcuri, R. Bruno, and P. Bevilacqua, "Influence of the optical and geometrical properties of indoor environments for the thermal performances of chilled ceilings," *Energy and Buildings*, vol. 88, pp. 229–237, Feb. 2015, doi: [10.1016/j.enbuild.2014.12.009](https://doi.org/10.1016/j.enbuild.2014.12.009).
- [28] S. Khare, M. Dell'Amico, C. Knight, and S. McGarry, "Selection of materials for high temperature sensible energy storage," *Solar Energy Materials and Solar Cells*, vol. 115, pp. 114–122, Aug. 2013, doi: [10.1016/j.solmat.2013.03.009](https://doi.org/10.1016/j.solmat.2013.03.009).